Research Article

Milan Dragoljevic*, Salvatore Viscuso, and Alessandra Zanelli

Data-driven design of deployable structures: Literature review and multi-criteria optimization approach**

https://doi.org/10.1515/cls-2021-0022
Received Sep 15, 2020; accepted Jan 28, 2021

Abstract: Classification and development of the deployable structures is an ongoing process that started at the end of 20th century and is getting more and more attention throughout 21st. With the development of the technology, constructive systems and materials, these categorizations changed – adding new typologies and excluding certain ones. This work is giving a critical review of the work done previously and on the change of the categories. The special interest is given to the pantographs (or scissor structures) and the Zeigler's dome as the form of their application. It is noticeable that after its introduction in 1977, the dome was a part of the initial classification, but with the time it lost its place. The reason for this is the introduction of more efficient scissor dome structures. However, perhaps with the use of data-driven design, this dome can be optimized and become relevant again.

The second part of the paper is dedicated to the development of the structural optimization algorithm for pantograph structures and its application on the example of Zeigler's dome. Besides the direct analysis, the final part includes the generative optimization algorithm which could help to a decision-maker in the early stages of the design to understand and select the options for the structure.

Keywords: deployable structures, classification, pantographs, Zeigler's dome, scissor mechanism, deployable dome, structural optimization, generative algorithm

***Corresponding Author: Milan Dragoljevic:** Politecnico di Milano, Dept. of Architecture, Built Environment and Construction Engineering Via Ponzio 31, 20133 Milan, Italy;
Email: milan.dragoljevic@polimi.it
Salvatore Viscuso, Alessandra Zanelli: Politecnico di Milano, Dept. of Architecture, Built Environment and Construction Engineering Via Ponzio 31, 20133 Milan, Italy

** Paper included in the Special Issue entitled: Shell and Spatial Structures: Between New Developments and Historical Aspects

1 Introduction

1.1 Deployable structures

Among the architectural structures, there are special ones that have the ability to change their shape, position in space and to adapt to external conditions. These are called adaptive and morphing structures. A special case of these structures which have a single degree of freedom and only two possible configurations (compact and deployed) are called deployable structures. The compact and deployed configurations are defined a priori and thus the structure is not conceived to respond or adapt to real-time changing scenarios, nor is designed to be used with different conditions in a same context [1]. This is performed as a response to a variable number of requirements: emergencies, special functions or changes of the environments. The other names of these structures are erectable, expandable, extendible, developable or unfurlable structures [2].

The use of deployable structures is a part of human society for a long time. Shelters that are easy to be transported and assembled were part of the exploration or the big movement of the tribes. Also, the military during the campaigns required sheltering on different terrains. Applications range from the Mongolian yurts to the velum of the Roman Coliseum, from Da Vinci's umbrella to the folding chair [3]. They were used whenever there was a need for a temporary enclosure. However, the academic interest in the topic began in the second half of the 20th century. Zuk and Clark published in 1970 their book Kinetic Architecture that was the first important focus on the topic [4]. Part of their references is coming from the 1960s: for example Rowan J. Progressive architecture – p. 93 [5].

Similar to the historical application, the structures today are also utilized for temporary needs. These include emergency situations sheltering, events organization or as a response to the change of the environment. All the mentioned situations require objects which will have a shorter use period compared to the conventional edifices. Because of this, construction time should also be shortened. Considering the emergencies, the utilization time and conditions are unpredictable, so the adaptability and possibility to re-deploy in a short time if needed plays a key role. The events can be organized as repetitive or on different locations, that is why the time for deployment and transport is very important.

Figure 1: POLIMI and IFRC, T2 Multipurpose collective shelter

Figure 2: Chuck Hoberman, Iris Dome Project, Interior perspective;1994

Considering the work on the comprehensive classification of different types of deployable structures, the examples started to show up from the 1980s [6]. After that, there was a big break until the 21st century, when the topic returned to focus and new attempts to classify general deployable structures showed up.

On the other hand, for the classification of specific types, the work was more continuous. The partial classifications presented on the chronology below (Figure 3) are compared with the general classifications and therefore observed in the same period. The first partial classification after the 1980s is a historical survey of cable and membrane roofs by Forster [7], published in 1994 and then deepened two years later in 1996 by Mollaert [8] with the classification of the membrane roofs. In 2001, Friedman publishes the doctoral thesis containing the review of deployable structures [9]. Yet, this review is focused on architectural and civil engineering applications and she specifies that it is not a comprehensive work. She publishes a similar review in 2011. Doroftei and Doroftei published in 2014 another short review of deployable structures [10]. Their classification contains 4 categories: spatial bar structures, foldable plate structures, strut-cable systems and membrane systems. However, in their work, they focus mostly on the first two classes. Puig *et al.* review deployable booms and masts [11]. This work classifies them as: inflatable, telescopic, coilable, shape-memory composite booms and deployable truss structures. Environmental performance as the criteria for classification is adopted by Ramzy and Fayed in 2011 [12]. They divide deployable structures into the following classes: skin-unit systems, retractable elements, revolving buildings and biomechanical systems. Santiago-Prowald and Baier focus on space antennas in their work from 2013 [13]. They distinguish different approaches in the deployment of them.

One of the first comprehensive classifications was done by Carlos H. H. Merchan in his Master thesis published 1987 for the Massachusetts Institute of Technology (MIT) [14]. The first level division in this case is between strut and surface elements. Linear elements as struts can resist different types of load (tension, compression or bending). On the other hand, surface structures are continuous and certain of them resist only tension forces. Sliding mechanisms (umbrella type) are mentioned in this classification, but not in further work of other authors. As part of the surface elements, there are inflatable or pneumatic structures, although without the explanation are they air-inflated or air-supported. Despite the extensive work on covering different typologies of the deployable structures, some of them were not mentioned, although they were invented at the time of the writing classification – tensegrities, air-supported structures and sliding structures used for retractable roofs. This division also contains pantographs [15] under the name of scissor hinged mechanisms.

After this, the next steps in classification are done in the 21st century – starting from the year 2001. Charalambos Gantes created the first classification in our century [16]. His book Deployable Structures: Analysis and Design contains a critical overview of the deployable structures. The first

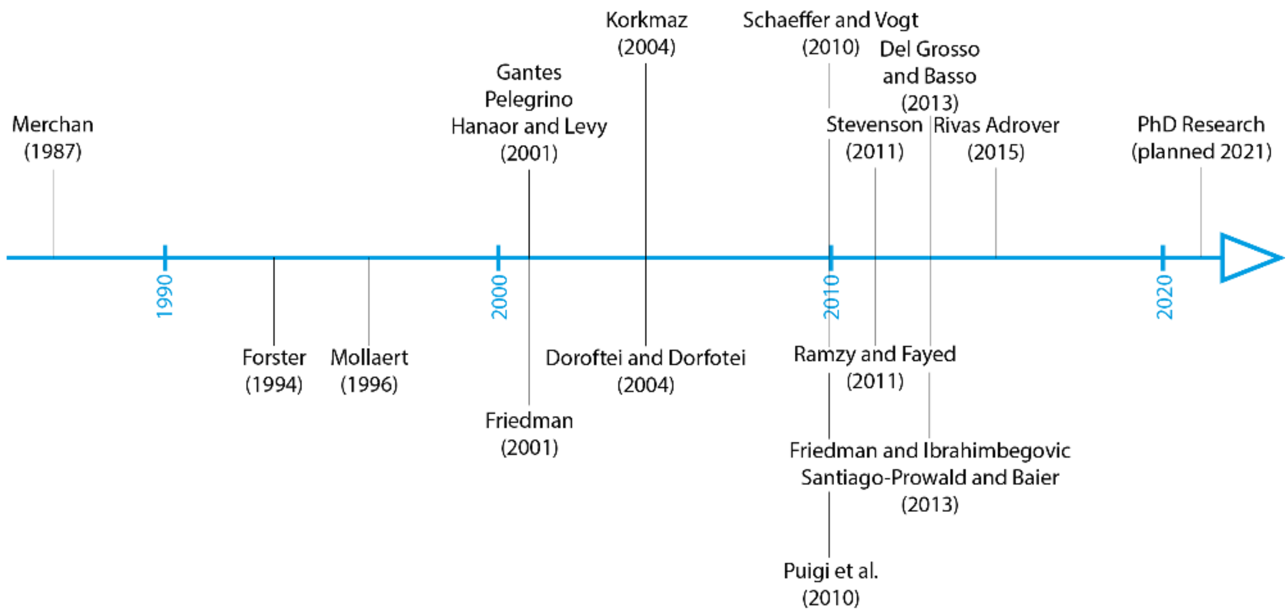

Figure 3: Chronological view of comprehensive and partial classifications of deployable structures published by now

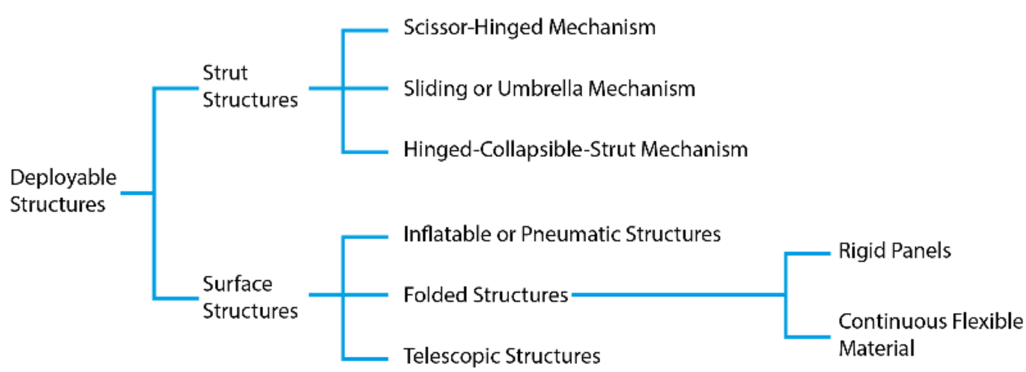

Figure 4: Merchan’s classification of deployable structures from 1987

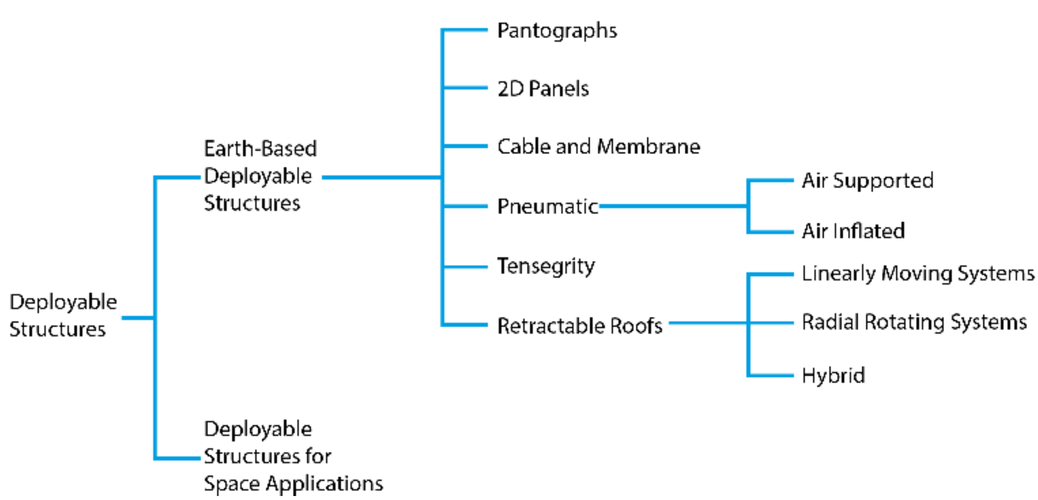

Figure 5: Deployable structures classification of Gantes in 2001

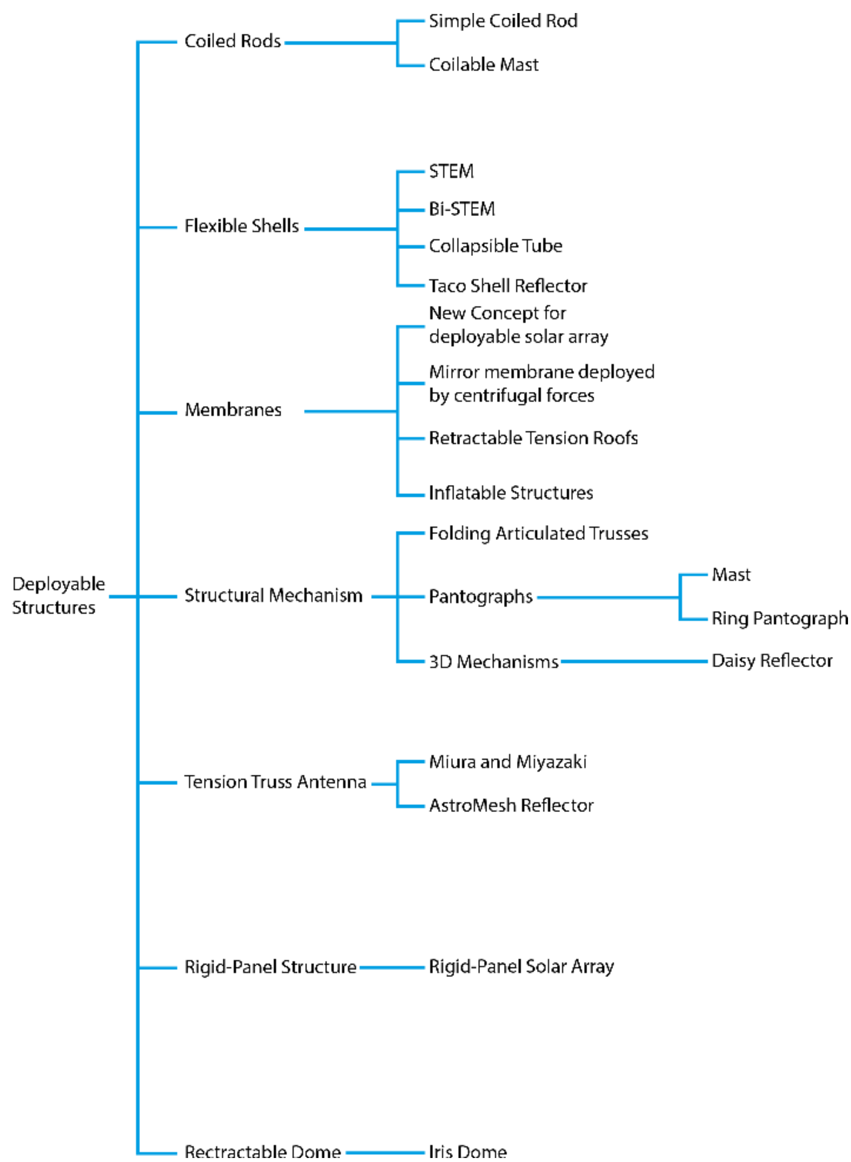

Figure 6: Pelegrino's classification of deployable structures from 2001

level of division is based on the application. Two classes are earth-based and spatial structures, depending on whether the self-weight plays an important role within the structure. Still, some of the structures from different classes have very similar kinematics and morphology, so the division is not so clean-cut [17]. Within the earth-based structures, there are pantographs, two-dimensional panels, cable and membrane structures, pneumatic structures, tensegrities and retractable roofs. It is important to notice that the subclasses here are structural forms for all the members besides the retractable roofs. They are defined by their application. Considering the space-based structures, there is no lower level of classification. In this classification, pantographs are classified under the earth-based deployable structures.

The next classification is made by the Sergio Pellegrino, done in the same year – 2001 [18]. It is published in the book Deployable Structures. In his work, prof. Pellegrino divides structures based on their kinetic motion and mechanism, not regarding their use. However, the majority of the structures are spatial ones. Certain specific structures, that were not mentioned earlier, are shown in his work: coilable masts, bi-stable structures and mirror membrane deployed by centrifugal force. Still, some of the fundamental structures are not explicitly mentioned or classified, such as tensegrities. Pellegrino classifies pantographs as structural mechanisms and names two types of them: masts and ring pantographs.

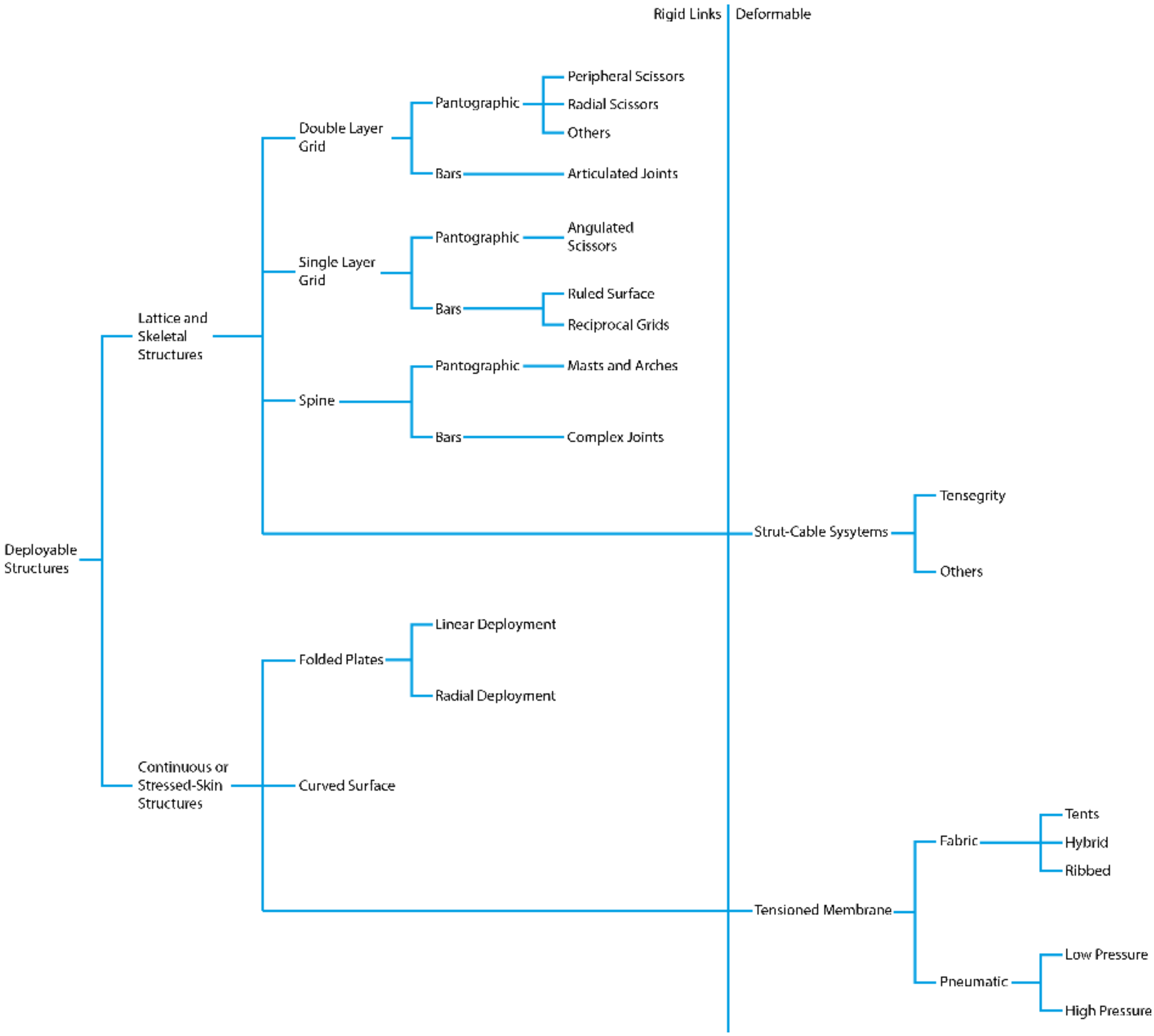

Figure 7: Hanaor's and Levi's classification from 2001

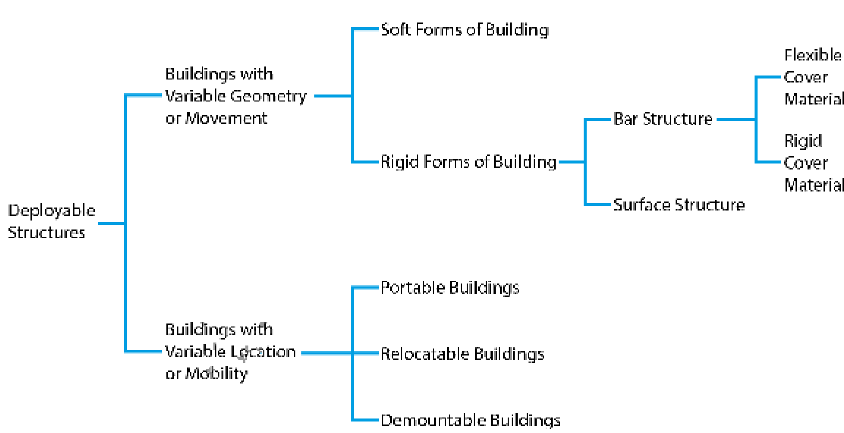

Figure 8: Classification of Korkmaz from 2004

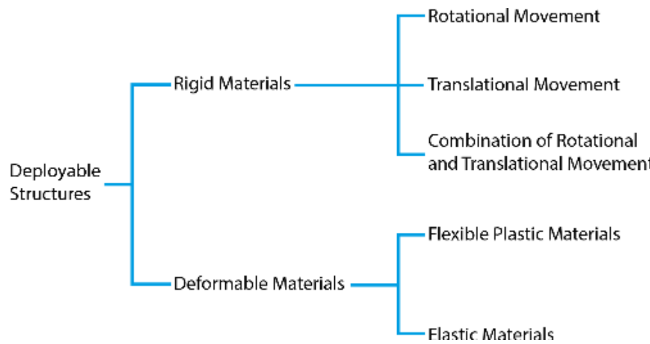

Figure 9: Classification of Schaeffer and Vogt from 2010

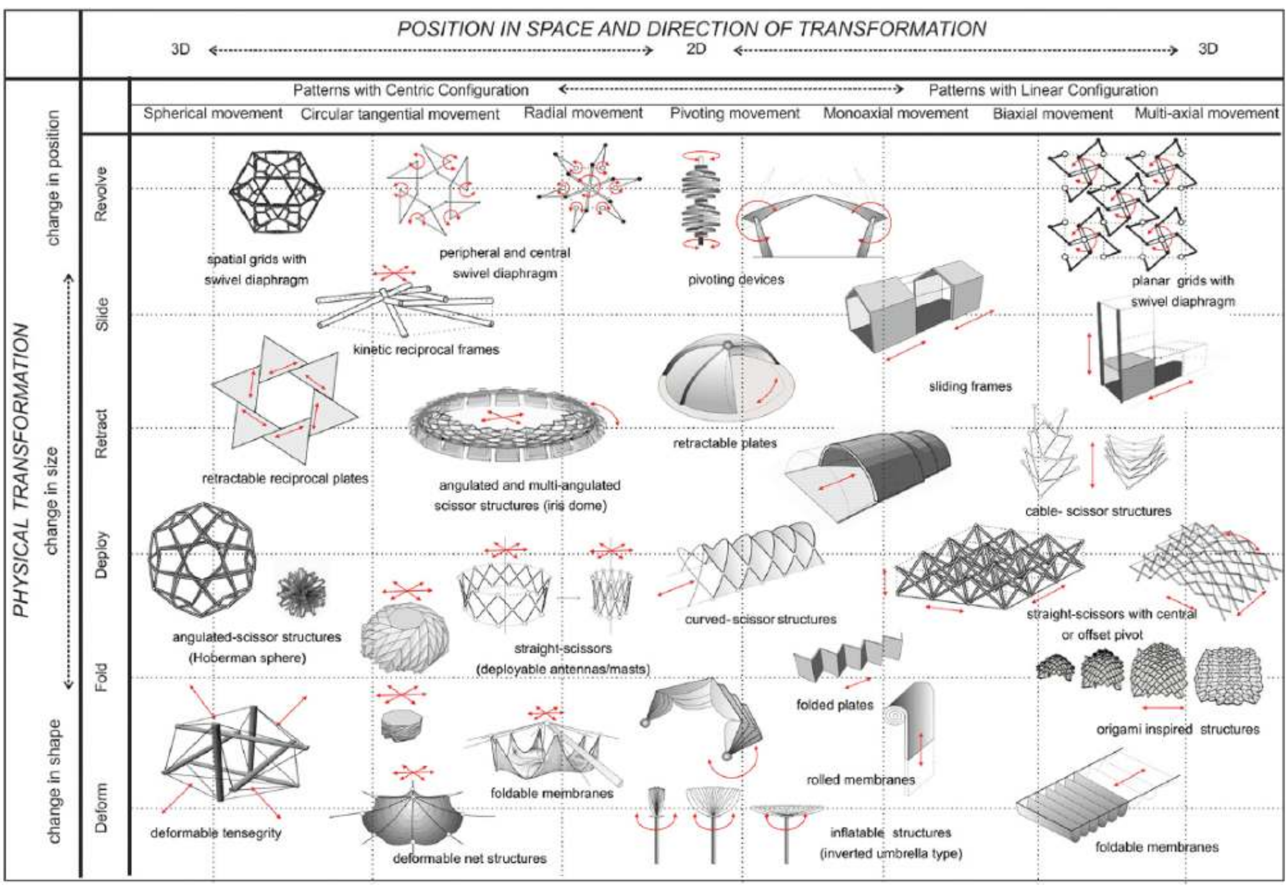

Figure 10: Classification by Stevenson from 2011

Hanaor and Levy created another classification during the same year, 2001 [19]. Their work is focused on architectural spaces, although they do not use applications as the criteria for the categorization. Classification, in this case, is a two-way division – morphological and kinematic. Considering the morphological criteria, the sub-classes are skeletal or lattice structures and continuous or stressed-skin structures. On the other division, kinetic sub-classes are rigid link systems and deformable components. There is also mentioned in a third class that combines skeletal and stressed-skin components, but it is not put in the table. Although very extensive and successful, when observed from today's perspective the classification lacks some types of the structure that were invented after 2001. Also, some deployable structures did not show up even though they existed in the time of writing, such as STEM or coilable structures. In this classification, pantographs are not in a single spot, but they are one of the subclasses for certain types of layer grids and spine. So the scissor shows up as peripheral, radial and other as the pantographic subtype of the double layer grid. Angulated scissors are a pantographic subtype for the single-layer grids. In the end, masts and arches are pantographic subtypes of spines. Considering the kinetic division, all pantographs are under the category of rigid links.

Korkmaz created the next classification in 2004 [20]. It was focused on the deployable structures applied in architecture. The definition by Fox and Yeh served as the initial point for classification. They stated that kinetic architecture comprises buildings, or components, with variable location and mobility in space and/or variable configuration and geometry. This brings the concept of "time" as the crucial parameter for categorization. Because of this, the two initial classes are: buildings with variable geometry or movement and buildings with variable location or mobility. Prof. Korkmaz introduces pantographs as bar structures. In the general classification of structures, they are under buildings with rigid form as the part of the buildings with variable geometry or movement.

Classification by Schaeffer and Vogt [21] was published in 2010. It starts from differentiating movement of rigid materials and movement of deformable ones. On the next level, for the rigid material structures, the division was done based on the type of the movement (rotational, translational or combination of the two). Deformable material structures are classified considering whether they are plastic or elastic.

Stevenson created the next classification in a chronological view. It was done in 2011. Differentiation among structures is two dimensional [22]. The classification observes operations of the single parts in relation to the movement of the whole structure. The author is not using a material to define classes in the division, focusing instead on the transformations: deforming, folding, deploying, retracting, sliding and revolving. Considering the issues in this approach, pneumatic structures were not included in the table and there is no differentiation between air inflated and air-supported structures. Stevenson classifies different types of scissors. They are part of the "deploy" and "retract" category considering the physical transformation. The diversity of the shapes that the scissors can form can be seen through the fact that they are present in all subcategories considering the classification of position in space and direction of transformation.

Del Grosso and Basso started their classification from 2013 by referencing Hanaor and Levy's table. Their work is different because of the inserting structures not mentioned earlier by other authors: compliant mechanisms under deformable structures and morphing truss structures under rigid link structures. Following the approach of Hanaor and Levy, Del Grosso and Basso also classify scissor mechanisms under the rigid links category [1].

And the most recent classification comes from architect Esther Rivas Adrover in 2015 [23]. Although his book Deployable structures is not peer-reviewed, his work is extensive. As the first level of division, it is taken the way on which the deployable structures are developed: one category are those based on structural components of the deployable mechanisms (Structural Components), while the other are the structures inspired by other sources (Generative Technique). The first class is later subdivided to rigid deployable components, deformable deployable components, flexible deployables and combined deployables. The second class was subdivided on where does the inspiration for the structure comes from, so it contains origami paper pleat and biomimetics. In this classification, the scissors show up as the rigid structural components, under the category of lattice work.

As it can be noted, the scissors are one of the structures present from the first comprehensive classification and during all other versions. The system that pantographs use is known as the lazy tong system. The basic unit of the sys-

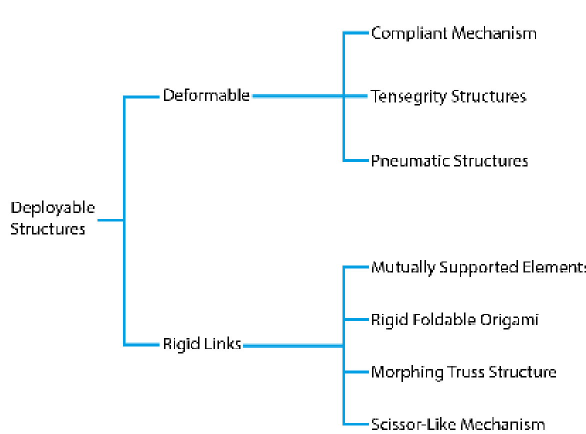

Figure 11: Classification by Del Grosso and Basso from 2013

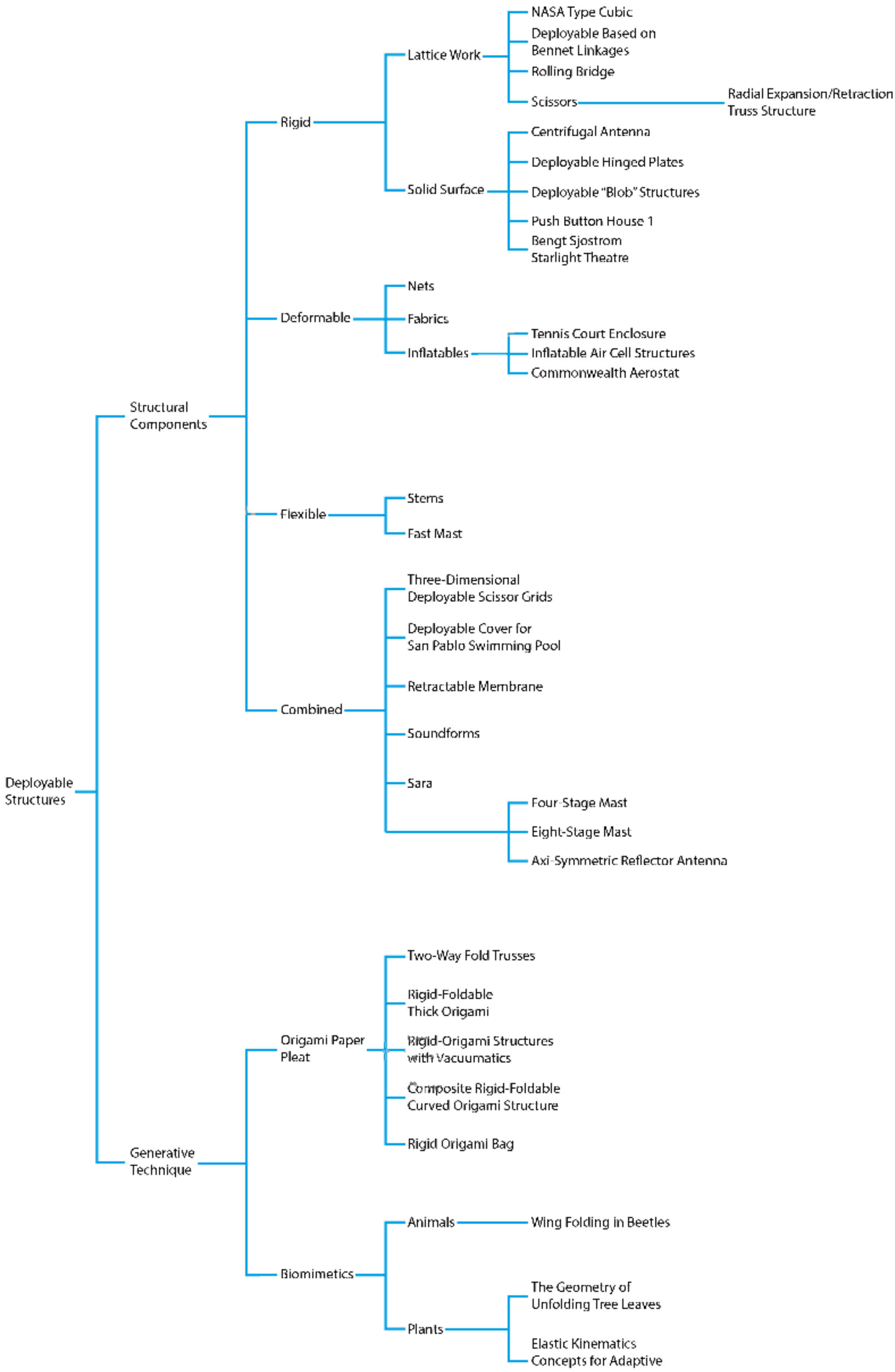

Figure 12: Classification by Rivas Adrover from 2015

Table 1: Evaluation of the double layer pantographic grids by Hanaor and Levy

Criteria	Evaluation
Design – Architectural flexibility	Flexible modular design is readily applicable. Large areas can be covered with relatively small modules connected on site.
Component uniformity	High component uniformity can be maintained, although doubly curved surfaces may require some variation in unit cell dimension.
Storage and transport – Stowed compactness	The structure folds to a compact bunch of bars. Compatible folding of the membrane covering needs to be considered.
Weight	Structural efficiency is medium to low, depending on the surface geometry, constituent units and bracing.
Maintenance (wear & tear)	Repeated deployment may cause significant wear and tear to the membrane and to connections.
Site inputs – Site preparation	Generally, self-supporting configurations can be designed, requiring minimal foundation and site preparation.
Connections	Degree of deployability is relatively high. Site connections involve connection of deployable modules and addition of bracing elements.
Complexity / reliability	Medium mechanical complexity. Articulated joints and hinges are relatively simple25. Human assistance in deployment is usually required.
Auxiliary equipment	No auxiliary equipment is required other than relatively light lifting equipment to assist in deployment and folding.

Table 2: Inclusion of the scissor structures, Zegiler's dome and dome in the general sense in the classifications over the years

	Merchan (1987)	Gantes (2001)	Pellegrino (2001)	Hanaor and Levy (2001)	Korkmaz (2004)	Schaeffer and Vogt (2010)	Stevenson (2011)	Del Grosso and Basso (2013)	Rivas Adrover (2015)
Scissor structures	included	included	included	Included	included	included	included	included	included
Zeigler's dome	included	included	included						
Dome					included	included	included	included	included

tem is called a scissor-like element (SLE). It is made out of two bars and a joint that is connecting them [3]. These elements can be added to each other to form parallel or curved systems. However, these structures require additional stabilizing elements like cables or other locking devices [10]. The other option in stabilizing is adding the internal layer of SLEs and the creation of the double-layer grid. In their work, Hanaor and Levy evaluated the double layer pantographic grids based on their predefined criteria for deployable structures.

The other thing to notice is that although the Zeigler's dome as a typology is present in the earliest classifications, the recent ones are not focusing on it. Zeigler's dome is the first example of a dome structure done with the double layer grid of pantographs. It is patented in the 1977 year [24]. The reason could be the structural inefficiency of the first versions of the dome. The problems were coming from residual stress and bending of the elements. Considering the general shape, the dome (defined as a semi-sphere) keeps the high efficiency of the sphere considering the surface area to volume ratio. That means that the biggest volume can be enclosed with the minimum surface. This property is in line with the intention of the algorithm to optimize the material use, so besides the use of the minimum acceptable cross-sections the covering membrane encloses the maximum possible volume.

This paper aims to examine the possibilities of the use of Grasshopper with Karamba in the process of optimization of scissor structures. The presented procedure could be used as a useful design tool in the early design stage.

2 Methods

For enabling better control over the design process, it is used parametric design software Grasshopper with structural calculations plug-in Karamba. The base 3D modeling software within which they work is Rhinoceros 3D. Thanks to this approach, the whole early-stage process of design is parametrized and gives full control to the designer. The design process is divided into two parts: the first allows the parametrized control over the dimensions, shape, and subdivision of the general structure and the second one which performs structural calculations and confirms the stability of the construction and resistance of the materials.

As already mentioned, the sample for testing the algorithm is selected Zeigler's dome. In the first part of the algorithm, the properties of the geodome are defined. For generating the initial structure, it is needed the radius, class (icosahedron/octahedron/tetrahedron) and frequency (level of the division of the geodome). In the following steps, the lines of geodome are transformed into a scissor structure. A double structure is used because a single layer dome does not have structural stability. This scissor structure is used for defining the rodes and the covering membrane. This part of the algorithm provides information about the weight, volume and area of the structure. Also, the length of the rodes can be checked in this step.

The second part of the algorithm is focused on structural calculations. The plug-in Karamba requires the specially defined model – adjusted to its specifications and limitations. This is a prerequisite for the use of any FEA software [25]. In terms of modeling geometry, it is needed to define the membrane as the mesh surface and the rods as straight lines. Karamba uses the mesh to define a "shell" element and the lines for the "beam" ones.

The main challenge of this approach is in the difference in the algorithms used for the membrane and the rods. Karamba allows the use of an algorithm for large deformations in the cases where elements have small dimensions – as in the case of the covering membrane (whose thickness is significantly less compared to other dimensions). However, rods are going through the deformation defined by the first-order theory for small deformations. Because of this, it is needed to calculate the elements separately. However, this leaves the question of the load transfer from one element to another.

The classical linear theory of elasticity is used for small displacements of the deformable body. This means that the positions of the points in deformed state are close to their initial positions. However, in large deformation analysis, the domain of the body is changing continuously, as well as its boundary conditions and the external loads [26]. For the point to reach its final position at the moment t it is needed to pass through different positions in time, starting from 0 and going through Δt, $2\Delta t$, $3\Delta t$, etc. These positions are obtained through incremental method of the analysis. With the algorithm based on large deformations theory, deforming body is evaluated in equilibrium positions for every given moment. Moreover, every next moment is calculated in relation to the previous one and this process is repeated until the final state of the body is not reached.

Since the membrane is the most external element, the snow or wind is applying force directly to it. The membrane as the element is supported along the rod lines. They are defined as supports within the algorithm for the membrane

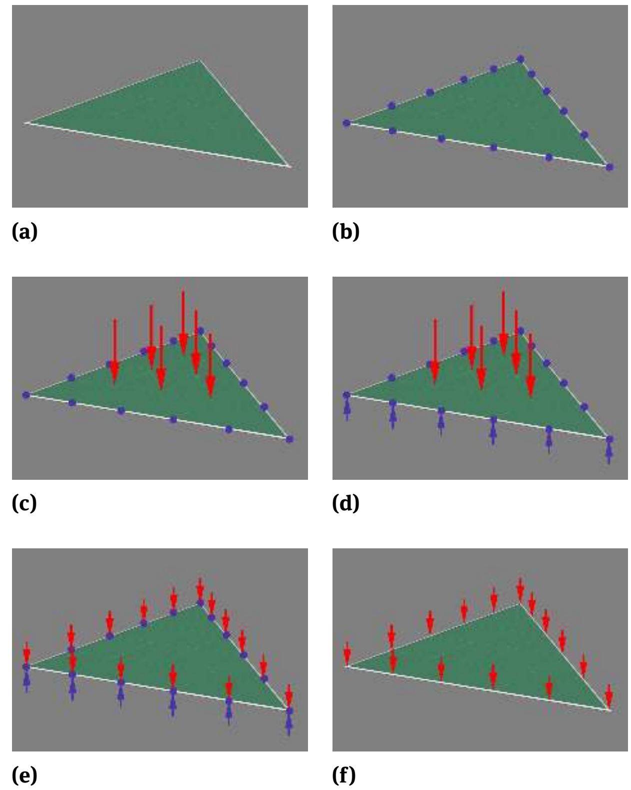

Figure 13: a) Schematic view of a single field of the dome: the green mesh is a membrane envelope and white tubes are the poles, b) Blue points which are mesh vertices on the poles, observed as support points for the membrane mesh, c) Load applied on the membrane mesh with shown support points, d) Resistant forces at the support points, e) Equilibrium of the forces at the support points, f) Forces obtained from the equilibrium state for the support points that load the poles

large deformation. The algorithm allows obtaining the resisting forces at supports. These forces are the opposite vectors compared to the loads that the membrane transfer to the rods. Thanks to this, the loads applied to the rods are defined and applied within the algorithm for the first-order theory deformation. For the rods system, support points are nodes on the ground.

The application of wind and snow loads is based on Eurocode regulation EN 13782. However, the wind load is adjusted to the dome structure which is not covered in detail in the given document. For this is used regulation EN 1991-1-4. The coefficients for wind forces are included accordingly.

Materials are defined in the algorithm as well. For the rods, it is used Steel Q235-B (S235JR), while for the membrane PVC Extruded. The important properties are given in the table below (in the units used within the algorithm).

The next part of the calculations is dedicated to bending moment resistance verification. It is done through a

Table 3: Properties of the materials used for the structure

Material	Steel Q235-B (S235JR)	Extruded PVC
Young's modulus of elasticity	20 000 kN/cm^2	280 kN/cm^2
Shear modulus (taken as approximately 3/8 of Young's modulus)	7500 kN/cm^2	105 kN/cm^2
Specific weight	77.15 kN/m^3	13.63 kN/m^3
Yield strength	103.4 kN/m^2	8.14 kN/m^2

comparison of the maximum bending moment that the cross-section can resist and the maximum cross-section that is generated within the structure. The plastic section modulus needs to be calculated first and then using it, the maximum bending moment that poles can resist. Formulas are the following ones:

$$W = \frac{D^3 - d^3}{6}$$

$$M_{c,\,Rd} = \frac{W \cdot f_d}{Y_{M0}}$$

Where

- D is the external diameter of the pole
- d is the internal diameter of the pole
- Y_{M0} = 1.1 and represents a partial factor for the resistance of cross-sections
- f_d is the minimum yield strength and for the used material (steel Q235-B) equals to 235 N/mm^2

The final part of the work is multivariable and multiobjective optimization. For this task, it used plugin Octopus. The objectives of optimization are:

1. Minimizing displacement
2. Minimizing the weight of the structure
3. Maximizing the cross-section resistance to the bending moment

As the variables are used:

1. Frequency of the structure (number of division fields within the dome)
2. Poles cross-section – diameter and thickness

Because of the 3 optimization objectives, it is possible to use the 3-axis space to represent potential solutions. Thanks to this approach, it is possible for the decision-maker to analyze potential solutions and select the one which is appropriate considering the production capacities.

3 Results

The tested structure is an icosahedron. The initial dimensions of the elements are the following:

- Poles: Diameter = 3 cm; Thickness = 0.5 cm
- Membrane: Thickness = 0.45 mm

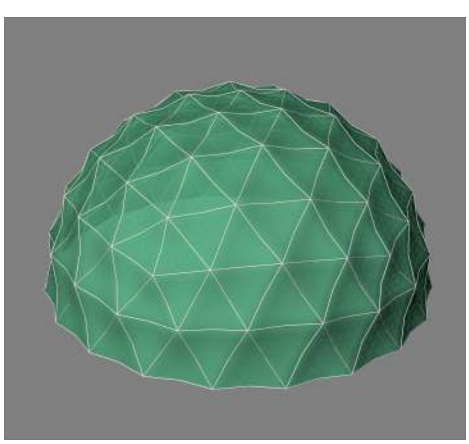

(a)

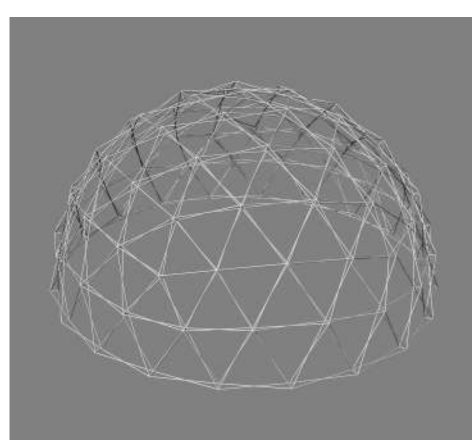

(b)

Figure 14: a) Initial dome membrane model; b) Initial scissor structure dome

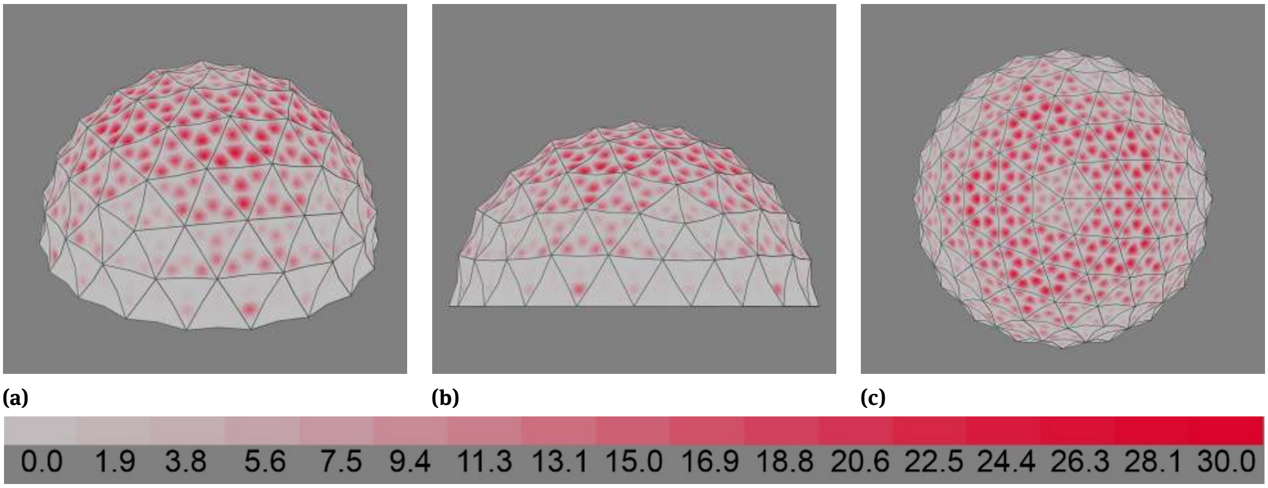

Figure 15: Fabric under the snow load (1.5 kN/m^2); a) 3D view, b) Side view, c) Top view. Maximum displacement: 27.67 cm

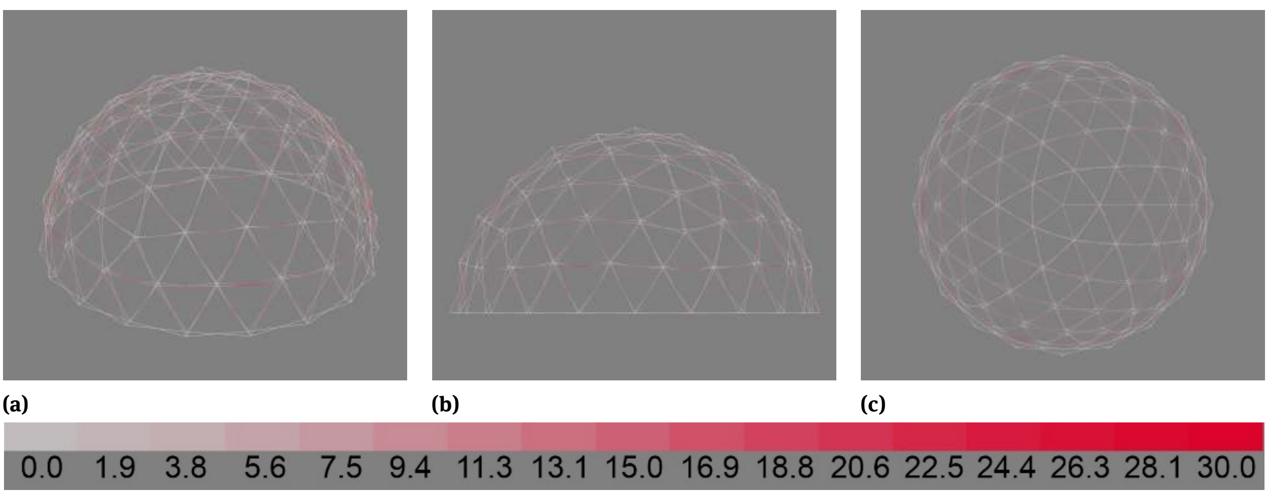

Figure 16: Pole structure under the snow load (1.5 kN/m^2). a) 3D view, b) Side view, c) Top view. Maximum displacement: 27.30 cm

3.1 Snow load

The first load case is the snow load. As the relevant standard, it is used Eurocode EN 1991-1-3. The selected location is Milan, Italy. The website www.dlubal.com allows automatic calculations of the snow and wind loads by the given standard for locations in different countries. Standard snow load for Milan by the EN 1991-1-3 equals 1.5 kN/m^2.

3.2 Wind load

Wind load is the second load case. Again, as the relevant standard, it is used Eurocode EN 1991-1-4. The selected location is again Milan, Italy and the same source is used for the load values. Standard wind load for Milan by the EN 1991-1-4 equals 0.39 kN/m^2.

3.3 Multiobjective optimization

Since the generated displacement and bending moment is bigger for the snow load, this case is used for structural optimization. The optimization includes multiple objectives and multiple variables. Considering the objectives, it is important to minimize displacement and the weight of the structure, while the acceptable bending moment for the cross-section has to be bigger than the maximum generated bending moment within the structure – for this condition, it is also better if this difference is bigger, but it is not decisive.

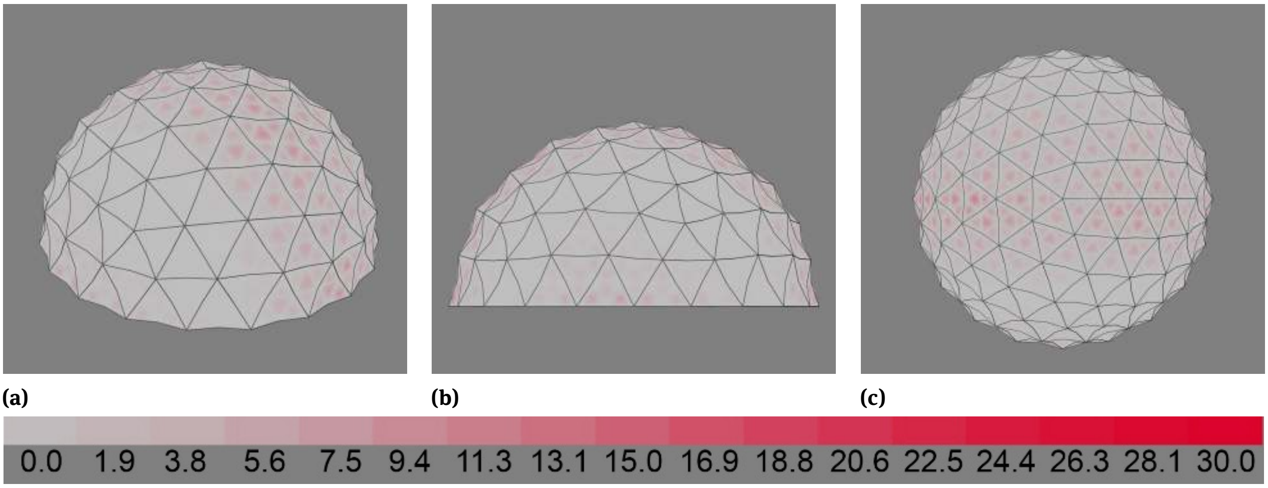

Figure 17: Fabric under the wind load (0.39 kN/m^2). a) 3D view, b) Side view, c) Top view. Maximum displacement: 12.52 cm

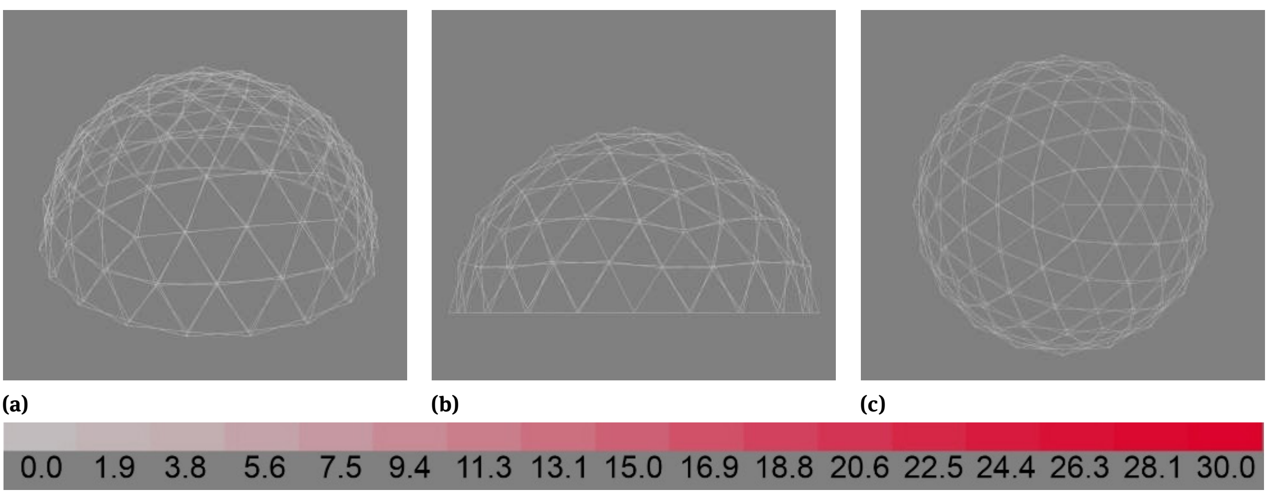

Figure 18: Pole structure under the wind load (0.39 kN/m^2). a) 3D view, b) Side view, c) Top view. Maximum displacement: 3.38 cm

On the graph below, these 3 values are shown as the axes:

– Displacement [cm]
– Weight [kg]
– M diff [kNm] – which is the difference between the maximum bending moment that the cross-section can resist and the maximum bending moment generated by the load

In the case of the third objective (moment difference), any solution where the resisting moment is smaller than the generated one has to be eliminated, so all the solution where this difference: Generated M – Resisting M is bigger than 0 are eliminated. Thanks to this, all the solutions represented with the points on the graph are acceptable and can be used for the selection of the most suitable one.

Considering the variables, there are cross-section (as diameter and the pole wall thickness) and frequency of the geodome (number of subdivisions). By the Grasshopper plug-in Octopus, they are not shown on the graph, but in the attached Table 4 there are values of variables for all generated solutions.

Considering the comparison of the design options and the values they generate, their impact is defined as equal. This means that all the parameters are equally weighted. In this case, different functions of linear standardization can be applied. Below in Table 5 are presented functions in the case of the maximization of the solution.

If the Row maximum linear standardization is applied with equally weighted parameters, each set of values can

Table 4: Input and output values obtained through the process of optimization (part of the data from the attachment)

Frequency	Diameter [cm]	Thickness [cm]	Displacement [cm]	Weight [kg]	Bending moment difference [kNm]
4	5.7	2.70	1.89	36433	−3.39
10	5.1	2.55	0.38	74918	−2.03
12	5.4	2.45	0.25	102053	−3.38
10	4.6	1.60	0.52	55428	−0.96
4	5.2	1.05	2.99	19817	−0.89
4	5.0	2.10	3.09	27509	−1.32
6	4.8	1.50	1.08	33494	−1.92
10	5.7	0.95	0.36	52137	−2.08
10	5.9	2.75	0.25	99646	−4.23
8	5.3	0.80	0.63	32810	−1.43
8	4.5	2.25	0.83	45945	−1.23
8	5.1	1.10	0.62	39995	−1.76
4	4.7	1.65	3.92	22814	−0.53
8	5.2	2.05	0.54	58474	−2.73
8	5.7	1.95	0.41	66153	−4.00

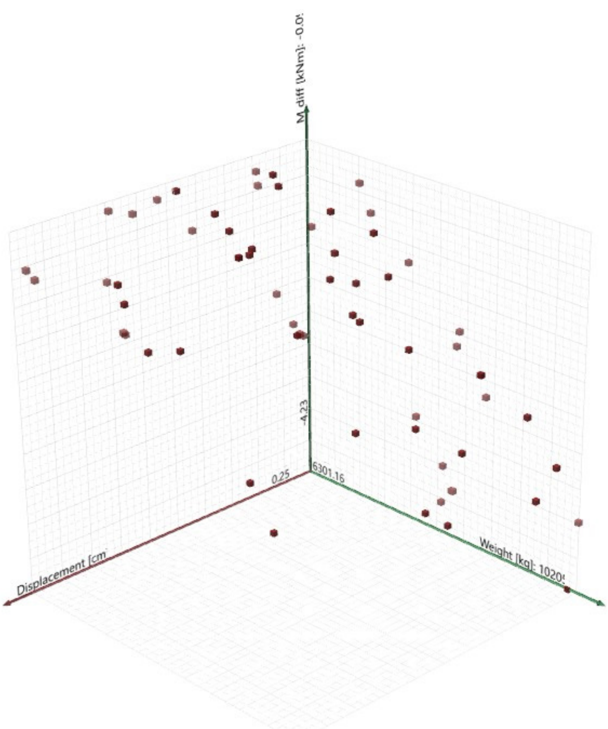

Figure 19: Octopus graph of multiobjective optimization

be awarded with the sum of row maximums:

$$C_i = \sum_{1}^{n} \frac{x_i}{x_{max}}$$

However, in this case, the solutions should be minimized, so every solution needs to be compared to the row minimum [27]:

Table 5: Functions of linear standardization

Standardization	Function
Row maximum	$\frac{x}{x_{max}}$
Ideal value	$\frac{(x - x_{min.id.})}{(x_{max.id.} - x_{min.id.})}$
Average value	$\frac{x}{x_{mean}}$
Interval standardization	$\frac{(x - x_{min.row})}{(x_{max.row} - x_{min.row})}$
Additive constraint	$\frac{x}{\sum x_{row}}$
Vector normalization	$\frac{x}{\sqrt{x^2}}$

$$C_i = \sum_{1}^{n} \frac{x_i}{x_{min}}$$

Thanks to this, Table 4 can be transformed to Table 6:

Table 6: Sum of equally-weighted row minimum standardizations

Frequency	Diameter [cm]	Thickness [cm]	C_i
4	5.7	2.70	10.20
10	5.1	2.55	5.78
12	5.4	2.45	6.95
10	4.6	1.60	5.10
4	5.2	1.05	13.17
4	5.0	2.10	14.06
6	4.8	1.50	6.46
10	5.7	0.95	4.56
10	5.9	2.75	7.03
8	5.3	0.80	4.51
8	4.5	2.25	5.93
8	5.1	1.10	4.91
4	4.7	1.65	16.96
8	5.2	2.05	5.76
8	5.7	1.95	5.92

4 Discussion

Considering the obtained results, two areas need to be further discussed: deformation of the membrane and the optimization process for the poles.

4.1 Membrane deformation analysis

As already noted, because the membrane is done of thin material, it was necessary to utilize a Large deformation theory algorithm. This algorithm is adding load increments that are scaled to 1/number of increments. For the given case, the number of increments is 1000.

However, during the application of the load, the membrane triangular field gets the shape of the underlying pole structure. Since the triangular field is formed by the scissor structures, the triangle does not have flat edges, but they are divided into two inclined parts. This causes the membrane to be divided into 4 small triangular fields (as seen in Figure 20). This creates folding lines within the same triangular field, which later impact the algorithm. The interpretation of the algorithm and the calculation software is that these folding lines are more resistant to deformation, therefore they remain less deformed.

This means that for the software, the folded membrane behaves similar to origami patterns that are already adopted as a method to strengthen the structure. On the Figure 21 below, it is represented the research in the use of Miura origami pattern for increasing the stiffness of the surface.

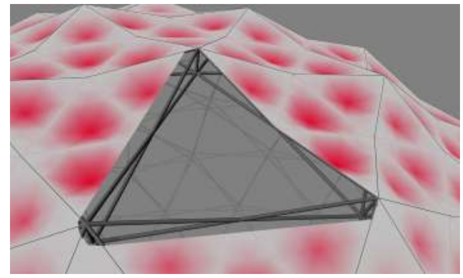

Figure 20: The shape of the membrane under the load

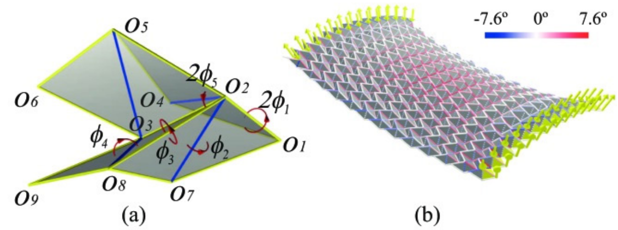

Figure 21: Increased structural stiffness of the folded edges (compared to the same material in the flat form) in the Miura origami pattern [28]

Further research could focus on physical testing at least a single field to understand does the folding lines provide the greater stiffness and how much if they do. The results could be compared with the virtual simulation.

4.2 The optimization process for the poles

As already explained, the final outcome for the poles structure is the optimization process. Since the production and construction of a pantograph dome include making many

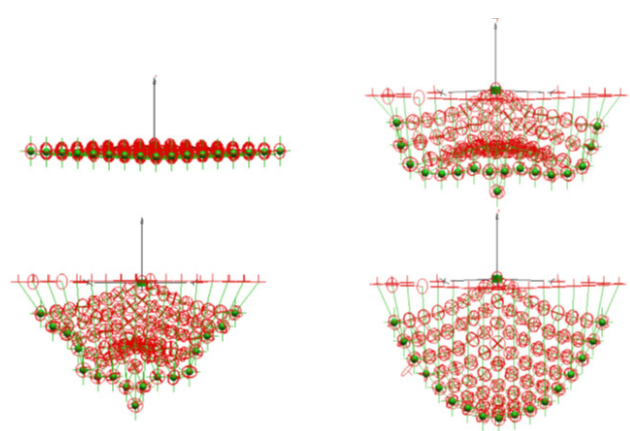

Figure 22: Application of MRA with different number of iterations [29]

Table 7: Maximum nodal displacement for different dimensions of the dome

Frequency	Diameter [cm]	Thickness [cm]	Maximum nodal displacement (II order theory) [cm]	Maximum nodal displacement (I order theory) [cm]	Difference [%]	Maximum rotation angle of a node (II order theory) [rad]	Maximum rotation angle of a node (I order theory) [rad]	Difference [%]
4	5.7	2.70	1.95	1.89	0.03	0.013	0.014	0.08
4	5.2	1.05	3.17	2.99	0.06	0.022	0.021	0.05
4	5.0	2.10	3.36	3.09	0.09	0.024	0.022	0.09
6	4.8	1.50	1.24	1.08	0.15	0.012	0.011	0.09
4	4.7	1.65	4.48	3.92	0.14	0.032	0.028	0.14
6	5.2	2.60	0.91	0.82	0.11	0.009	0.008	0.13
6	4.4	2.20	1.63	1.35	0.21	0.016	0.013	0.23
6	4.3	0.65	2.63	1.98	0.33	0.026	0.020	0.30
4	5.6	1.15	2.32	2.25	0.03	0.017	0.016	0.06
6	4.1	2.05	2.13	1.67	0.28	0.021	0.017	0.24
6	4.6	0.70	1.97	1.59	0.24	0.020	0.016	0.25
6	3.5	1.75	4.28	2.69	0.59	0.044	0.027	0.63
6	3.9	0.85	3.22	2.27	0.42	0.033	0.022	0.50
4	5.3	1.00	3.01	2.86	0.05	0.022	0.020	0.10
6	3.8	1.90	2.92	2.10	0.39	0.030	0.021	0.43
4	5.9	2.55	1.71	1.67	0.02	0.012	0.012	0.00
4	5.0	2.40	3.36	3.09	0.09	0.024	0.022	0.09
6	6.0	0.70	0.85	0.78	0.09	0.009	0.008	0.13
6	4.1	2.05	2.13	1.67	0.28	0.021	0.017	0.24
4	5.2	1.20	3.03	2.87	0.06	0.022	0.020	0.10
6	5.1	0.70	1.4	1.20	0.17	0.014	0.012	0.17
4	4.7	1.45	4.52	3.97	0.14	0.032	0.028	0.14
4	5.1	2.55	3.09	2.87	0.08	0.022	0.020	0.10
6	5.0	1.15	1.16	1.15	0.01	0.012	0.010	0.20
6	4.6	0.80	1.81	1.48	0.22	0.018	0.015	0.20
6	4.7	1.85	1.3	1.12	0.16	0.013	0.011	0.18
4	5.1	2.55	3.09	2.87	0.08	0.022	0.020	0.10
6	4.7	0.90	1.58	1.33	0.19	0.016	0.013	0.23
6	4.1	2.05	2.13	1.67	0.28	0.021	0.017	0.24
				Avg. difference	0.17		Avg. difference	0.19

decisions, the multiobjective optimization does not bring a single solution that is better than the others. Instead, it creates a matrix of connected starting variables and final values which can be evaluated by the decision-maker.

In this case, in Table 4, there are inputs frequency, diameter and thickness for the structure and results general displacement, the weight of the structure and bending moment difference (maximum generated bending moment – the maximum bending moment which the cross-section can resist). Bending difference is always set to be negative because the maximum generated bending moment has to be smaller than the bending moment which cross-section can resist.

Thanks to the presented information, the decision-maker can give “weight” to each result and compare or sort data and select the more suitable ones for production and construction.

Further research could go in the direction of checking the behavior of the real scissor models and comparison with the virtually obtained data.

The other important question for the optimization of the poles is their stability. Considering the instability of the model, use of the linear approach (first-order theory of deformation) does not provide the response on the stability of the system. The stability could be controlled through the two additional procedures.

The first useful procedure for this case could be the multi-body rope approach. By virtually loading nodes within the structural system, it is possible to bring it to the stable configuration. However, the form of the deployable structures is determined by the deployability mechanism as well, so perhaps the results cannot reach the perfectly optimized configuration as in the case with the ropes. Therefore, the mechanism design should be integrated with MRA for the best results.

Considering the second approach for checking the instability of the system, it can be done by applying the second-order theory algorithm and the comparison of the nodal displacement with the results obtained through first-order theory analysis. As already described in one of the previous chapters, the second order theory is based on incremental application of the loads on the structure. It takes the structure through the intermediate states until reaching the final one. The final position of the structure is therefore the stable configuration considering the given loads.

When applying this algorithm on the initial structure (frequency of the geodome = 4; diameter of the pole = 3cm, wall thickness = 0.5cm), there is an issue of buckling in the case of the snow load. In this case, the compressive normal forces are too big and it causes buckling of the structural system. As the result, the algorithm is unable to calculate the behavior of the structure. In further research, with the changes in the diameter and wall thickness and through the application of the same approach, it is possible to minimize the nodal displacement values. Below is Table 7 with the maximum nodal displacement for different values of the diameter and wall thickness of the poles. Because of the complexity of the system, the II order theory analysis is performed for frequencies 4 and 6. Also, there is an issue of the system undergoing buckling (as the initial dimensions of the given system), so the procedure of looking for a minimum requires a second check is the system under buckling or not.

As it can be seen in the upper table the average difference in displacement between two approaches (I and II order theory) is 17% for maximum nodal displacement and 19% for the rotation angle.

Funding information: The authors state no funding involved.

Author contributions: All authors have accepted responsibility for the entire content of this manuscript and approved its submission.

Conflict of interest: The authors state no conflict of interest.

References

[1] Del Grosso A, Basso P. Deployable Structures. Advances in Science and Technology. 2012;83:122–31.
[2] Jensen FV. Concepts for retractable roof structures. PhD thesis; 2005.
[3] De Temmerman N. Design and analysis of deployable bar structures for mobile architectural applications. Vrije Universiteit Brussel; 2007.
[4] Zuk W, Clark RH. Kinetic architecture. Van Nostrand Reinhold Company; 1970.
[5] Rowan J. Progressive architecture. Philip H. Hubbard; 1968.
[6] Escrig F. Expandable space structures. Int J Space Struct. 1985;1(2):79–91.
[7] Forster B. Cable and membrane roofs – a historical survey. Struct Eng Rev. 1994;6:145–74.
[8] Mollaert M. Retractable membrane roofs. WIT Transactions on the Built Environment. WIT Press. 1996;21:407–17.
[9] Friedman N. Investigation of highly flexible, deployable structures: review, modelling, control, experiments and application. Budapest University of Technology and Economics; 2001.
[10] Doroftei I, Doroftei I–A. Deployable structures for architectural applications – a short review. Applied Mechanics and Materials. 2014; 658: 233–40.
[11] Puig L, Barton A, Rando N. A review on large deployable structures for astrophysics missions. Acta Astronautica. 2010; 67: 12–26.
[12] Ramzy N, Fayed H. Kinetic systems in architecture: new approach for environmental control systems and contextsensitive buildings. Sustain Cities Soc. 2011;1:170–7.
[13] Santiago–Prowald J, Baier H. Advances in deployable structures and surfaces for large apertures in space. CEAS Space J. 2013;5:89–115.
[14] Merchan CHH. Deployable structures. Massachusetts Institute of Technology; 1987.
[15] Kaveh A, Davaran A. Analysis of pantograph foldable structures. Comp & Struct. 1996;59(1):131–40.
[16] Gantes CJ. Deployable structures: analysis and design. WIT Press; 2001.
[17] Fenci GE, Currie NG. Deployable structures classification: A review. Int J Space Struct. 2017;32(2):112–30.
[18] Pellegrino S. (eds) Deployable Structures. International Centre for Mechanical Sciences (Courses and Lectures). Springer; 2001.
[19] Hanaor A, Levy, R. Evaluation of Deployable Structures for Space Enclosures. Int J Space Struct. 2001;16:211–29.
[20] Korkmaz K. An analytical study of the design potentials in kinetic architecture. İzmir Institute of Technology; 2004.
[21] Schaeffer O, Vogt MM, Scheuermann A. MOVE: architecture in motion – dynamic components and elements. Birkhäuser. 2010.
[22] Stevenson CM. Morphological principles: current kinetic architectural structures. Adaptive Architecture. 2011; 1–12.
[23] Adrover ER. Deployable Structures. Laurence King Publishing. 2015.
[24] Zeigler TR. Collapsible self–supporting structure. Patent 3,968,808. 1976.
[25] Preisinger C, Moritz H. Karamba – A Toolkit for Parametric Structural Design. Struct Eng Int. 2014;24(2):217–21.
[26] Gomez Botero M. Finite element formulation for large displacement analysis. Universidad EAFIT; 2009.

[27] Lacidogna G, Scaramozzino D, Carpinteri A. Optimization of diagrid geometry based on the desirability function approach. Curved Layered Struct. 2020;7:139–52.
[28] Wei ZY, Guo ZV, Dudite L, Liang HY, Mahadevan L. Geometric Mechanics of Periodic Pleated Origami. Phys Rev Lett. 2013;110:215501.
[29] Manuello A. Multi–body rope approach for grid shells: Form–finding and imperfection sensitivity. Eng Struct. 2020; 221.